WELDING RESEARCH

SUPPLEMENT TO THE *WELDING JOURNAL*, FEBRUARY 1997
Sponsored by the American Welding Society and the Welding Research Council

Submerged Arc Fillet Welds between Mild Steel and Stainless Steel

The classical analysis for ferrite, assuming equal contributions from the two base metals totaling 30% dilution, is often not valid

BY D. J. KOTECKI AND V. B. RAJAN

ABSTRACT. Submerged arc fillet welds between mild steel and Type 304 stainless steel, made with ER309L wire, may contain no ferrite and be at risk of hot cracking, or they may be sufficiently diluted that they transform to martensite with both hot cracking risk and low ductility. This situation is most prevalent when direct current electrode positive (DCEP) polarity is used and when the flange is the mild steel part of the T-joint. A flux that adds chromium to the weld can somewhat alleviate this tendency. Direct current electrode negative (DCEN) polarity greatly reduces this tendency by limiting dilution. Fillet weld compositions and dilutions are obtained for a number of welding conditions and fluxes.

Introduction

When joining mild steel to austenitic stainless steel, it is common to assume equal contribution to dilution from each member of the joint and total base metal dilution of about 30% into the weld (Ref. 1). Therefore, for joining mild steel to Type 304 stainless steel, Type 309 or 309L filler metal seems like a safe choice to provide a small amount of ferrite in the otherwise austenitic weld metal, thereby providing maximum assurance of freedom from hot cracking (Refs. 1–3). While Type 312 stainless steel filler metal or a nickel-based alloy filler metal might also be considered, these filler metals are more expensive and not as readily available as ER309L for submerged arc welding. As a result, fabricators often prefer to use ER309L, at least for weldments that will not experience prolonged high-temperature service.

The interested reader may wish to consult the compilation by Lundin (Ref. 4) of some 160 references concerned with dissimilar welds. While most of these are directed at problems along the fusion boundary, especially in joining $2^1/_4$ Cr-1 Mo steel to austenitic stainless steels, there are a number of references included that address weld filler metal selection for joints of mild steel to stainless steel.

Figure 1 presents a very standard analysis of the situation when joining mild steel to 304 stainless steel, using the Schaeffler diagram (Refs. 1–3, 5, 6). The mild steel base metal (represented by the filled square located along the left edge of the diagram) has a significant nickel equivalent by virtue of its carbon content but has a nearly zero chromium equivalent. The 304 base metal (shown as the open square near the center of the diagram) typically would produce a small amount of ferrite if it were simply melted by gas tungsten arc (GTA) welding, for example, although this base metal type seldom exhibits ferrite in the wrought condition due to hot working after casting. The fifty-fifty mix of 304 and mild steel is represented by the midpoint of the tie line between the two base metals and would be expected to consist largely of martensite. The 309L filler metal (represented by the plus sign to the right of center in Fig. 1) is connected to the fifty-fifty base metal mix by a second tie line. The expected weld metal composition (shown as the filled circle) with 30% total dilution from the two base metals is found at 30% of the distance from the filler metal composition to the fifty-fifty base metal mix composition, and the weld metal would be expected to consist of a small amount of ferrite in an austenite matrix.

The Schaeffler diagram is considered outdated for ferrite predictions (Ref. 7) because it does not consider the effects of nitrogen, because it presents its predictions in "percent ferrite" (it has proven

KEY WORDS

Carbon Steel
Dilution
Dissimilar Metals
Fillet Welds
Flux Effect
Polarity Effect
Stainless Steel
Submerged Arc
Wire Feed Speed

D. J. KOTECKI and V. B. RAJAN are with The Lincoln Electric Company, Cleveland, Ohio.

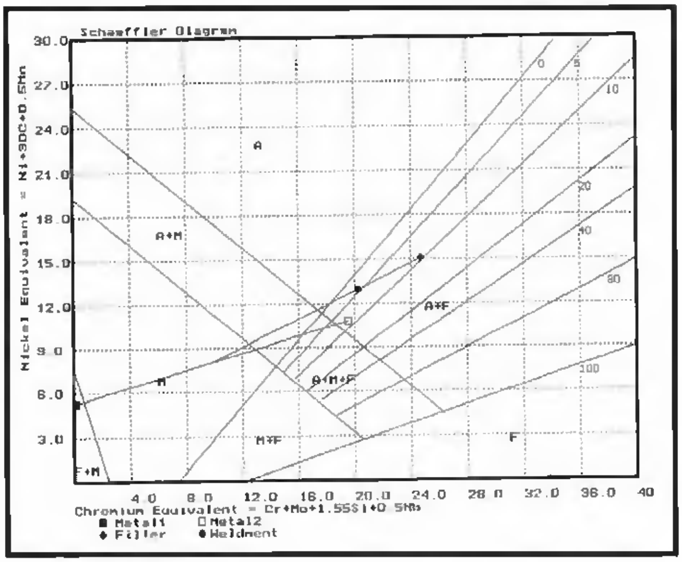

Fig. 1 — Typical Schaeffler diagram analysis of a mild steel to Type 304 stainless steel weld with 309L filler metal, using FERRITE PREDICTOR software (Ref. 6). Metal 1 (■) is mild steel, Metal 2 (❑) is Type 304 steel, Filler (✚) is 309L and Weldment (●) is the predicted fillet weld metal at 30% dilution.

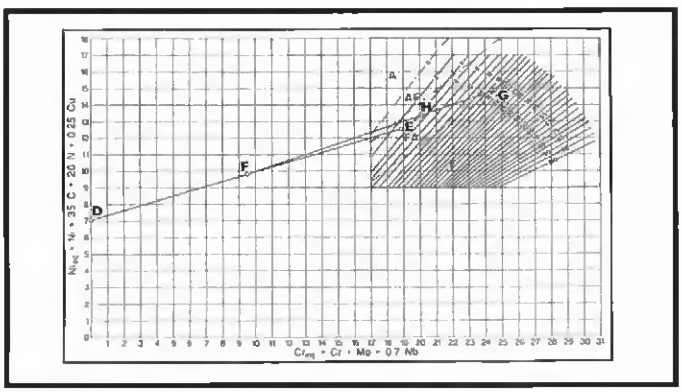

Fig. 2 — Typical WRC-1992 diagram analysis of a mild steel to Type 304 stainless steel weld with 309L filler metal (Ref. 7). In the figure, "D" represents the mild steel, "E" the 304 steel, "F" an equal mix of mild steel and 304 steel, "G" the 309L filler metal, and "H" the predicted fillet weld metal at 30% dilution.

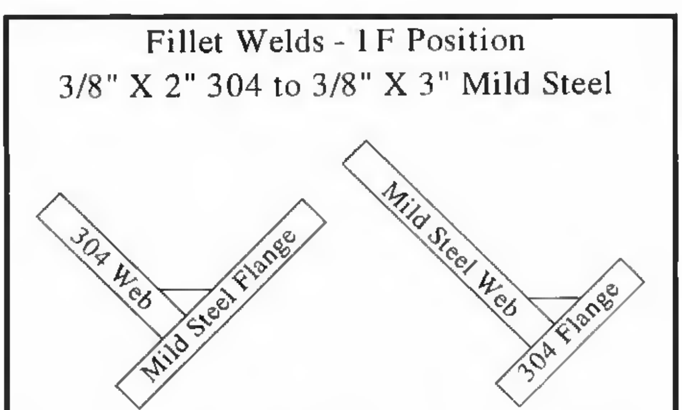

Fig. 3 — Schematic of fillet weld tests.

impossible to reach agreement on the "percent ferrite" in a given weld metal) and because it considers manganese to be part of the nickel equivalent (which it clearly is not). Nevertheless, it continues to find applications in dissimilar metal joining because it makes reasonable predictions concerning the stability of austenite vs. transformation to martensite. The WRC-1992 diagram, currently considered to be the most accurate for predicting ferrite content (Ref. 7), can be used with dissimilar metal joints but does not currently make predictions concerning martensite. An analysis similar to that of Fig. 1 is repeated with the WRC-1992 diagram (with extended axes according to Ref. 7) in Fig. 2, and again, the prediction would be that a small amount of ferrite would be obtained in an otherwise austenitic deposit. In either case, the weld ought to be free of cracking. It should be recognized that solidification as primary ferrite is the characteristic necessary to eliminate hot-cracking tendencies (Ref. 8), not the presence of ferrite at room temperature. However, the presence of a small amount of ferrite at room temperature generally corresponds to solidification as primary ferrite, as indicated by the dashed line in Fig. 2 that separates compositions that solidified as primary ferrite (Regions FA and F) from compositions that solidified as primary austenite (Regions AF and A).

Because the 304 stainless steel is found to lie in the FA region of Fig. 2 (primary ferrite solidification), dilution from the 304 steel has an essentially neutral effect on whether the weld solidifies as primary ferrite or primary austenite. It is the dilution from the mild steel side, far out into the region of primary austenite solidification in Fig. 2, that tends to eliminate ferrite in the weld (at lower levels of dilution) and to promote martensite (at higher levels of dilution).

The prediction of a weld consisting of a small amount of ferrite in austenite, however, depends upon the assumption of about 30% total dilution with approximately equal contributions from the two base metals (*i.e.*, 15% from the mild steel and 15% from the 304 steel). Experience has shown that this is a fairly accurate prediction for shielded metal arc welding (SMAW), so Type 309L covered electrodes are commonly and successfully applied to such joints. However, the economical production of long fillet welds between stainless steel and mild steel, such as in the manufacture of "water walls" made of stainless steel pipes and mild steel bars, leads to a preference for submerged arc welding (SAW) instead of SMAW. Whereas 30% dilution is commonly and consistently obtained in SMAW, the dilution obtained with SAW can vary greatly, depending upon the specific combination of wire diameter, wire feed speed (current), polarity and travel speed chosen. Dilution over 50% can occur in SAW (Refs. 3, 9). One can see from Fig. 1 or 2 that dilution in excess of 40%, when a 309L filler metal is used to join mild steel to 304, could lead to a ferrite-free weld sensitive to hot cracking. Furthermore, Fig. 1 would predict that such a weld at about 50% dilution, or at lower dilution when the dilution came more from the mild steel side than from the 304 side, would contain considerable martensite.

Both ferrite-free welds containing hot cracks and highly martensitic welds were encountered while assisting a fabricator in the development of procedures for production of water walls. As a result, a systematic study was undertaken to examine more fully the effect of welding parameters on dilution and the resulting weld microstructure when using SAW to make fillet welds between mild steel and 304 stainless steel with ANSI/AWS A5.9 Class ER309L welding wire.

Experimental Materials

Mild steel bars of $^3/_8$ in. (9.5 mm) by 3 in. (76 mm) cross section and Type 304 stainless steel bars of $^3/_8$ in. (9.5 mm) by 2 in. (51 mm) cross section were used as base metals for this study. The filler metal was ER309L, $^3/_{32}$ in. (2.4 mm) diameter. The compositions and Ferrite Numbers (calculated from composition using the WRC-1992 diagram) of these three materials are given in Table 1.

Three fluxes were used in the study. American Welding Society standards do not provide classifications for fluxes for SAW of stainless steels; therefore, it is necessary to describe the fluxes in terms of chromium recovery and welding characteristics. Flux ST-100 (hereafter referred to as the "chromium-compensating flux") performs well only in DCEP welds. It tends to produce a small increase in all-weld-metal (six or more layers of buildup) chromium content as compared to wire chromium content (about 0.5–1.0% Cr when the filler wire is ER309L) (Ref. 9). Flux 802 (hereafter referred to as the "highly basic chromium-free flux") is usable DCEP, DCEN or AC and tends to produce a loss of about 1% Cr in the all-weld metal as compared to the wire composition (Ref. 9). Flux A-100 (hereafter referred to as the "chromium-adding flux") is usable DCEP, DCEN or AC and can produce an all-weld-metal chromium gain of as much as 6%, depending upon the ratio of flux melted to wire melted, when ER309L filler metal is used (Ref. 9).

Table 1 — Materials Used

	Metals		
	Mild Steel Base Metal	Type 304 Base Metal	ER309L Wire
C, %	0.166	0.037	0.024
Mn, %	0.36	1.67	2.09
P, %	0.007	0.031	0.020
S, %	0.026	0.023	0.011
Si, %	0.05	0.56	0.52
Cr, %	0.08	18.43	23.96
Ni, %	0.09	8.80	13.27
Mo, %	0.03	0.26	0.04
Cu, %	0.04	0.29	0.37
N, %	—	0.04	0.043
WRC-1992 FN	—	7.3	13.9

Fluxes

ST-100 Chromium compensating
A-100: Chromium adding
882: Highly basic chromium free

Table 2 — Experimental Welding Conditions

Constant Conditions

Electrode diameter	3/32 in. (2.4 mm)
Electrode extension	1.25 in. (32 mm)
Welding voltage	34 V (DCEP and DCEN)
Flange material	Mild steel or 304 stainless
Electrode position	Aligned with, and perpendicular to, joint centerline

Variable Conditions

Wire Feed Speed, in./min (m/min)	Travel Speed, in./min (mm/min)	Approximate Current, A(a) DCEP	DCEN
60 (1.5)	9 (230)	200	160
90 (2.3)	13.5 (340)	270	210
120 (3.0)	18 (460)	340	260
150 (3.8)	22.5 (570)	420	320
180 (4.6)	27 (690)	490	380

(a)The controlled variable is wire feed speed, not current.

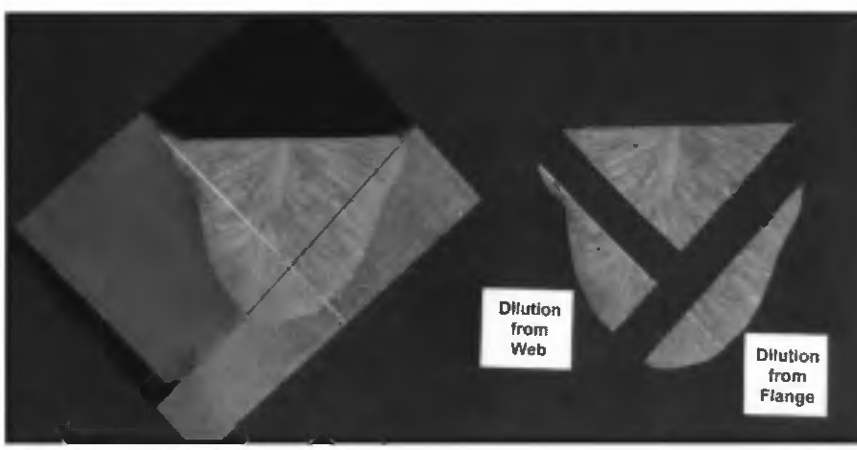

Fig. 4 — Photomacrograph of a cross section of fillet weld BWF120. Left — as taken; right — after being cut along scribe lines prior to the pieces being weighed for dilution calculation. Not all of the flange thickness is shown; the flange and web are both $^3/_8$ in. (9.5 mm) thick.

Experimental Procedure

A fixture was used to restrain the base metals and position them with the joint

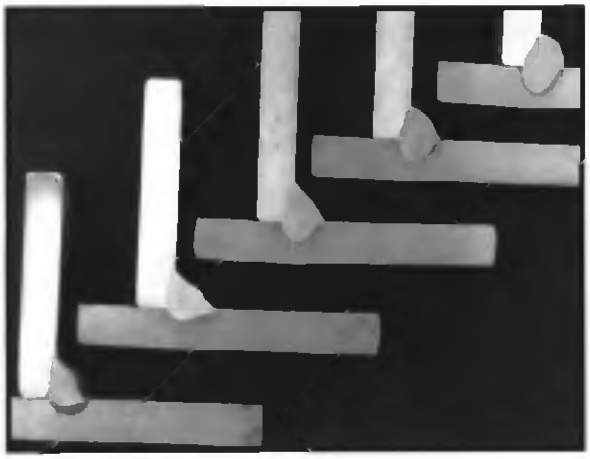

Fig. 5 — Photomacrograph of cross sections of DCEP fillet welds BWF115, BWF117, BWF119, BWF121 and BWF123 (from lower left to upper right). All welds were made with the chromium-adding flux, with mild steel as the flange and with increasing wire feed (increasing current and travel speed) from lower left to upper right. Penetration and dilution increase with increasing wire feed speed.

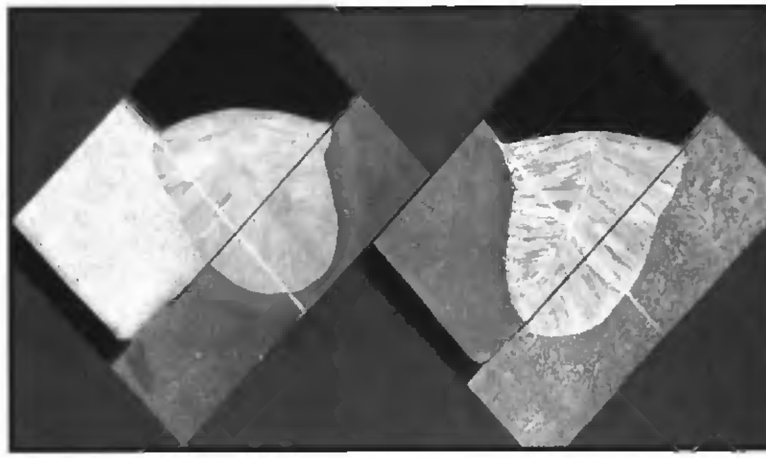

Fig. 6 — Photomacrograph of cross sections of DCEP fillet welds BWF109 (mild steel flange — left) and BWF110 (304 flange — right) under otherwise identical conditions. Note that, although the top surface of each weld is symmetric about the weld centerline, the root penetration is strongly deflected toward the mild steel side of the joint. This is typical of DCEP welds in this study. Not all of the flange thickness is shown; the flange and web are both $^3/_8$ in. (9.5 mm) thick.

in the flat (1F) position. Under each welding condition, a single-pass fillet weld was executed two ways: once with mild steel as the flange and 304 stainless as the web, and a second time with 304 as the flange and mild steel as the web, as illustrated in Fig. 3. The electrode centerline was always aligned with the joint centerline and was maintained perpendicular to it.

For each flux and each flange/web combination, five fillet welds were made according to the conditions listed in Table 2. Under all five conditions, the ratio of wire feed speed to travel speed is constant ($6^2/_3$:1), resulting in a calculated fillet weld size of 0.3 in. (7.6 mm) for all of the welds. Each weld was approximately 12 in. (300 mm) in length.

After a given weld was completed, a 2-in. (50-mm) length was cut from near the midlength. From this piece, chips were machined from the weld surface for carbon and sulfur analysis. The weld surface was then ground flat and analyzed for other elements by optical emission spectrophotometry. On this same surface, before chemical analysis, the weld Ferrite Number was measured with a Fischer Feritscope Model MP-3, calibrated according to ANSI/AWS A4.2.

Adjacent to the piece chosen for chemical analysis, a cross section was prepared for metallographic examination. This was macroetched with a solution of 200 g of ferric chloride, 300 mL of HNO_3 and 100 mL of water, to reveal the extent of penetration. The original base metal surfaces were scribed on this etched surface. To permit dilution calculations, a photomacrograph at about 5X magnification was taken and then cut apart along the fusion line and along the scribe lines to separate the area contributed by the filler metal, the area contributed by the web and the area contributed by the flange, as illustrated in Fig. 4. The three pieces of the photomacrograph of a given weld were individually weighed on a precision analytical balance to the nearest 0.0001 g. The photographic weight of each base metal area, as a percent of the total fusion zone area weight, was then calculated as the

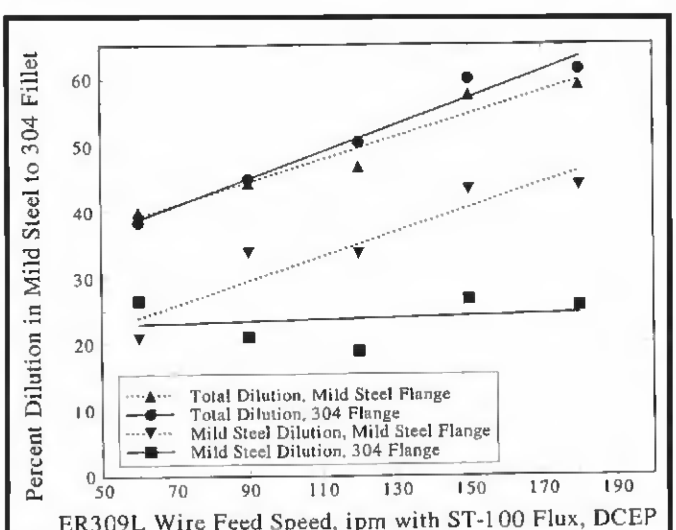

Fig. 7 — Effect of wire feed speed on dilution in DCEP welds with the chromium-compensating flux.

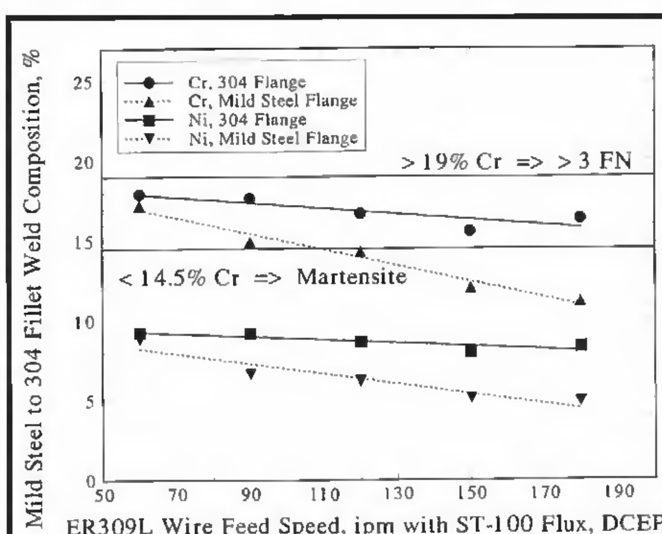

Fig. 8 — Effect of wire feed speed on fillet weld chromium and nickel contents in DCEP welds with the chromium-compensating flux.

Table 3 — Fillet Weld Test Results: SAW with 3/32 in. (2.4 mm) ER309L Wire at 34 V, 1.25 in. (32 mm) Electrode Extension

Sample No.	Wire Feed Speed in./min	Wire Feed Speed mm/min	Travel Speed in./min	Travel Speed mm/min	Flange[a]	% Dilution from Mild Steel	% Dilution from Stainless Steel	C	Mn	P	S	Si	Cr	Ni	Mo	Cu	FN[b]	Comments
Chromium-Compensating Flux, DCEP Polarity																		
BWF105	60	1524	9.0	229	MS	20.8	19.2	0.069	1.75	0.022	0.016	0.56	17.22	8.85	0.06	0.23	0.8	Convex
BWF106	60	1524	9.0	229	304	26.6	11.8	0.088	1.84	0.024	0.016	0.55	17.94	9.27	0.06	0.24	1.7	Convex
BWF107	90	2286	13.5	343	MS	33.7	10.7	0.085	1.57	0.020	0.018	0.48	14.94	6.64	0.04	0.20	0.0	Convex
BWF108	90	2286	13.5	343	304	21.0	23.9	0.064	1.76	0.023	0.017	0.53	17.65	9.17	0.08	0.25	2.1	
BWF109	120	3048	18.0	457	MS	33.6	13.0	0.088	1.48	0.018	0.020	0.45	14.32	6.18	0.04	0.19	1.6	
BWF110	120	3048	18.0	457	304	18.9	31.5	0.076	1.65	0.021	0.017	0.50	16.69	8.64	0.09	0.23	1.1	
BWF111	150	3810	22.5	572	MS	43.1	14.4	0.105	1.29	0.016	0.020	0.38	12.04	5.11	0.04	0.17	(61.7)	Martensite, hot crack
BWF112	150	3810	22.5	572	304	26.7	33.2	0.064	1.52	0.020	0.018	0.47	15.58	8.02	0.10	0.23	0.2	
BWF113	180	4572	27.0	686	MS	43.7	15.2	0.114	1.21	0.015	0.020	0.37	11.19	4.89	0.03	0.16	(67.1)	Martensite, hot crack
BWF114	180	4572	27.0	686	304	25.7	35.6	0.064	1.55	0.020	0.017	0.48	16.36	8.34	0.12	0.24	1.1	
Chromium-Adding Flux, DCEP Polarity																		
BWF115	60	1524	9.0	229	MS	25.8	11.8	0.070	1.61	0.022	0.016	0.56	20.15	9.02	0.06	0.24	10.1	
BWF116	60	1524	9.0	229	304	19.6	19.1	0.091	1.61	0.022	0.016	0.56	21.21	9.82	0.07	0.24	11.6	
BWF117	90	2286	13.5	343	MS	25.6	16.1	0.077	1.44	0.020	0.018	0.51	18.33	6.83	0.05	0.21	2.1	
BWF118	90	2286	13.5	343	304	21.5	21.1	0.065	1.59	0.022	0.016	0.56	20.83	9.37	0.08	0.24	13.4	
BWF119	120	3048	18.0	457	MS	35.0	20.7	0.083	1.29	0.018	0.019	0.46	14.84	6.23	0.06	0.20	0.4	
BWF120	120	3048	18.0	457	304	20.8	29.7	0.069	1.47	0.021	0.017	0.50	17.92	8.39	0.10	0.23	3.4	
BWF121	150	3810	22.5	572	MS	38.8	17.3	0.096	1.23	0.016	0.019	0.40	13.51	5.27	0.05	0.17	(57.3)	Martensite
BWF122	150	3810	22.5	572	304	33.8	24.4	0.074	1.38	0.019	0.019	0.45	16.14	6.47	0.09	0.21	0.7	
BWF123	180	4572	27.0	686	MS	41.7	20.2	0.106	1.19	0.015	0.020	0.39	12.85	5.14	0.04	0.17	(63.1)	Martensite
BWF124	180	4572	27.0	686	304	23.1	35.5	0.069	1.47	0.021	0.019	0.49	16.97	8.41	0.12	0.23	2.1	Slag in root
Chromium-Adding Flux, DCEN Polarity																		
BWF125	60	1524	9.0	229	MS	2.4	22.2	0.043	1.87	0.028	0.016	0.70	25.98	12.20	0.06	0.30	35.0	Lack of root penetration
BWF126	60	1524	9.0	229	304	10.6	2.8	0.053	1.73	0.024	0.015	0.62	23.44	10.86	0.04	0.26	20.9	Lack of root penetration
BWF127	90	2286	13.5	343	MS	5.9	18.2	0.050	1.77	0.023	0.015	0.63	23.65	11.43	0.06	0.28	21.3	
BWF128	90	2286	13.5	343	304	13.6	10.0	0.053	1.71	0.023	0.015	0.60	22.39	10.74	0.06	0.27	15.9	
BWF129	120	3048	18.0	457	MS	10.7	24.1	0.060	1.62	0.022	0.016	0.57	20.74	10.06	0.07	0.25	9.7	
BWF130	120	3048	18.0	457	304	23.0	9.4	0.071	1.58	0.021	0.016	0.56	20.44	9.69	0.05	0.24	8.5	
BWF131	150	3810	22.5	572	MS	9.6	20.7	0.052	1.69	0.022	0.018	0.62	21.28	10.73	0.08	0.28	10.6	
BWF132	150	3810	22.5	572	304	23.9	13.1	0.055	1.58	0.021	0.018	0.57	20.50	9.83	0.08	0.25	9.1	
BWF133	180	4572	27.0	686	MS	11.4	30.2	0.056	1.61	0.021	0.019	0.57	20.05	9.97	0.09	0.26	8.1	Undercut
BWF134	180	4572	27.0	686	304	30.0	23.0	0.075	1.48	0.020	0.018	0.50	18.26	8.94	0.07	0.23	3.2	Undercut
Highly Basic Chromium-Free Flux, DCEN Polarity																		
BWF135	60	1524	9.0	229	MS	4.0	24.4	0.036	1.83	0.021	0.013	0.67	20.12	11.32	0.07	0.30	4.6	Slag in root
BWF136	60	1524	9.0	229	304	18.3	4.1	0.069	1.66	0.019	0.014	0.62	18.43	10.76	0.07	0.26	1.6	Undercut
BWF137	90	2286	13.5	343	MS	8.1	20.9	0.047	1.81	0.019	0.014	0.63	19.60	10.99	0.06	0.28	3.5	
BWF138	90	2286	13.5	343	304	18.2	11.3	0.059	1.77	0.018	0.014	0.58	18.01	10.14	0.05	0.27	1.5	
BWF139	120	3048	18.0	457	MS	10.8	26.4	0.051	1.77	0.019	0.014	0.59	19.21	10.73	0.07	0.28	2.8	
BWF140	120	3048	18.0	457	304	21.2	10.2	0.069	1.56	0.017	0.017	0.55	16.93	9.49	0.05	0.24	0.8	Hot crack
BWF141	150	3810	22.5	572	MS	9.1	27.3	0.044	1.70	0.020	0.015	0.61	19.41	10.81	0.09	0.28	4.1	
BWF142	150	3810	22.5	572	304	20.6	19.8	0.050	1.64	0.019	0.015	0.57	18.33	10.26	0.07	0.27	1.9	Hot crack
BWF143	180	4572	27.0	686	MS	15.3	17.2	0.050	1.64	0.019	0.015	0.56	18.39	10.13	0.08	0.27	1.9	Undercut
BWF144	180	4572	27.0	686	304	27.8	15.0	0.081	1.46	0.015	0.016	0.48	15.61	8.80	0.05	0.22	0.0	Hot crack, undercut

(a) MS = Mild Steel. If the flange is mild steel, the web is 304; if the flange is 304, the web is mild steel.
(b) A FN in parentheses is falsely high due to martensite presence.

percent dilution from each base metal.

Note that it would also be possible to calculate the dilution contribution from each base metal from the weld metal nickel and chromium contents of each weld vs. the nickel and chromium contents of each base metal and of a corresponding all-weld-metal deposit. However, because the flux-to-wire ratio would change for each welding condition, and therefore the all-weld-metal composition would change for each welding condition, that method of calculating dilution would require a separate all-weld-metal sample for each individual welding condition, in addition to solution of two simultaneous equations with two unknowns. It was considered that the method of weighing cross-sectional areas of photomacrographs would be equally precise and involve considerably less labor.

The macrosections were also examined under a microscope, at 50X magnification, for hot cracks.

Experimental Results

Table 3 lists the individual welding conditions, calculated dilution, measured deposit chemical analysis, measured Ferrite Number and comments about the welds. For each series of welds, it can be seen that the dilution increases with increasing wire feed speed (increasing current), as would be expected.

With DCEP welding, which is usually

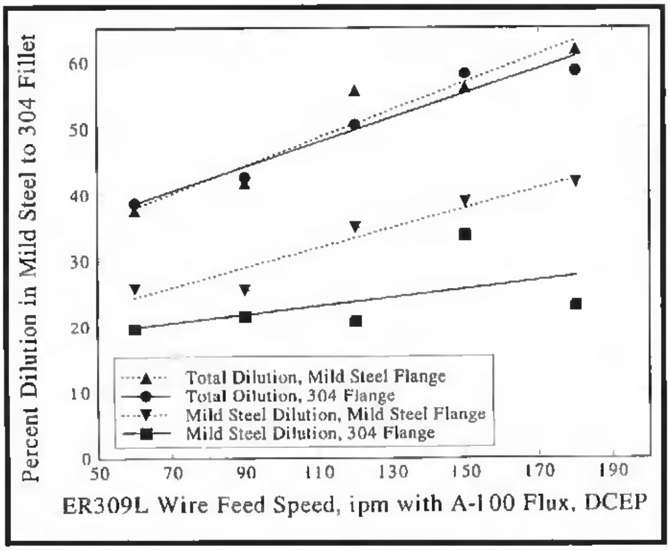

Fig. 9 — Effect of wire feed speed on dilution in DCEP welds with the chromium-adding flux.

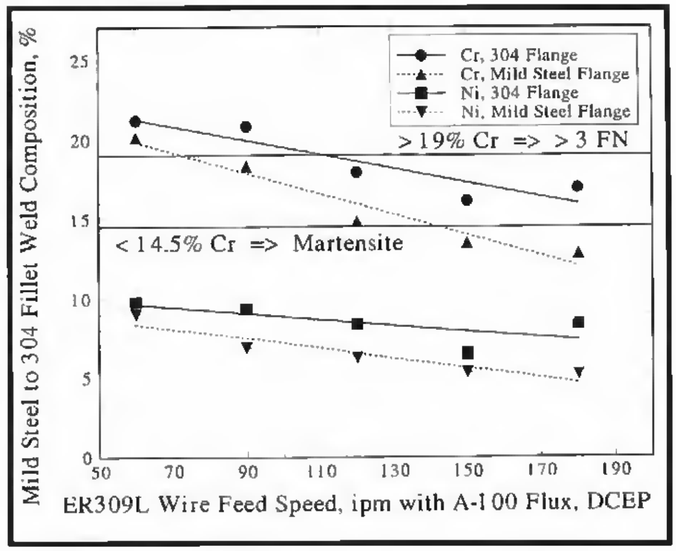

Fig. 10 — Effect of wire feed speed on fillet weld chromium and nickel contents in DCEP welds with the chromium-adding flux.

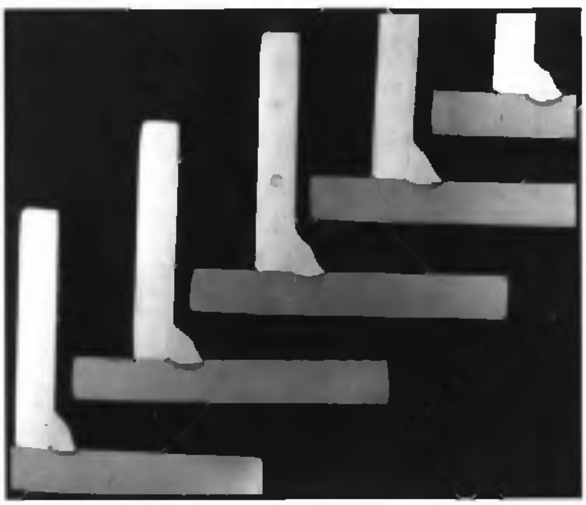

Fig. 11 — Photomacrograph of cross sections of DCEN fillet welds BWF135, BWF137, BWF139, BWF141 and BWF143 (from lower left to upper right). All welds were made with the highly basic chromium-free flux, with mild steel as the flange and with increasing wire feed speed (increasing current and travel speed) from lower left to upper right. Penetration beyond the root is little affected by increasing wire feed speed.

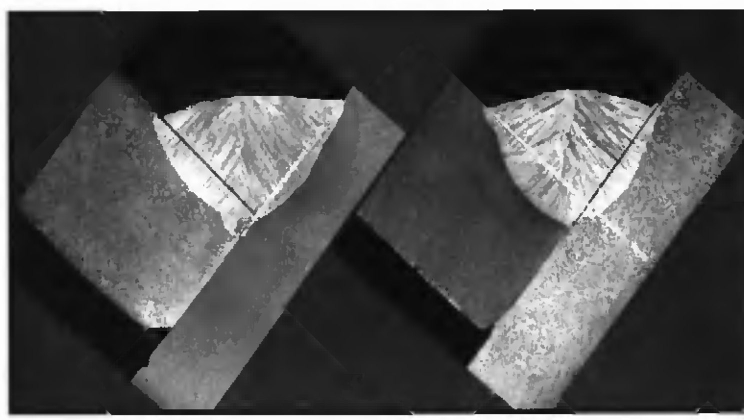

Fig. 12 — Photomacrograph of cross sections of DCEN fillet welds BWF131 (mild steel flange — left) and BWF132 (304 flange — right) under otherwise identical conditions. Note that penetration is greater on the web side in both cases. This is typical of DCEN welds of this study. Not all of the flange thickness is shown; the flange and web are both $^3/_8$ in. (9.5 mm) thick.

preferred by the welding operator, total dilutions ranged from less than 40% to over 60%, with dilution from the mild steel side ranging from about 10% to over 40%. As expected, the chromium-adding flux results in more ferrite under a given welding condition than does the chromium-compensating flux. Because ferrite in the weld is desirable, the chromium-adding flux is therefore more tolerant of dilution from the mild steel side of the joint. In general, the weld Ferrite Numbers decrease with increasing dilution from the mild steel side, until martensite appears in the welds at high dilution. Because martensite is also ferromagnetic, it gives a (false) high Ferrite Number.

With DCEN welding, dilution is generally lower than that for DCEP. Several of the welds made with the highly basic chromium-free flux contain ferrite above 3 FN and no hot cracks, but there is a small margin of safety. On the other hand, all of the welds made with the chromium-adding flux contain considerable ferrite and no hot cracks. Therefore, this flux, when welding DCEN, allows a wide range of suitable welding parameters. However, DCEN welding is noted to produce occasional lack of root fusion (slag in the weld root) at very low wire feed speeds and occasional undercut at very high wire feed speeds (and high travel speeds).

The DCEP weld macrosections exhibit two phenomena that significantly change the classical analysis indicated in the Introduction. First, for the higher wire feed speeds (which would be desirable from a productivity viewpoint), penetration of the fusion zone extends well beyond the original root of the joint. In a fillet weld, when penetration extends well beyond the root, the flange becomes a

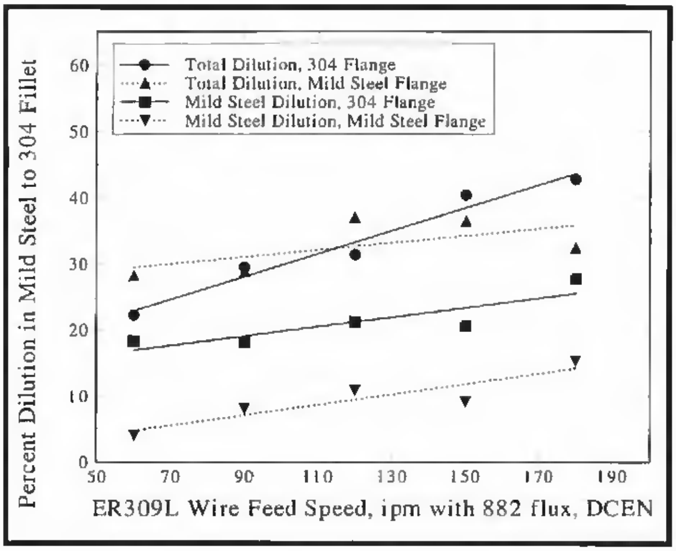

Fig. 13 — Effect of wire feed speed on dilution in DCEN welds with the highly basic chromium-free flux.

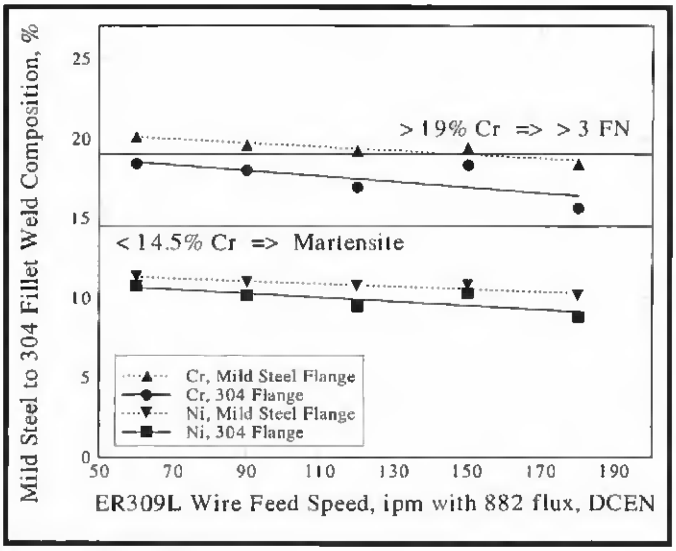

Fig. 14 — Effect of wire feed speed on fillet weld chromium and nickel contents in DCEN welds with the highly basic chromium-free flux.

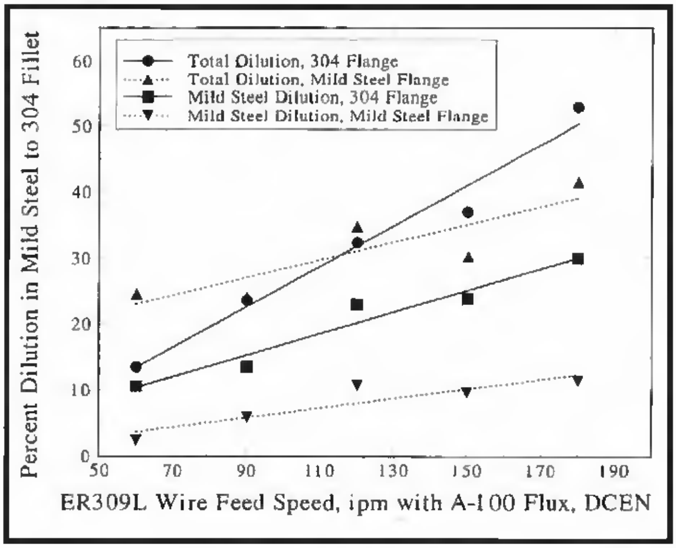

Fig. 15 — Effect of wire feed speed on dilution in DCEN welds with the chromium-adding flux.

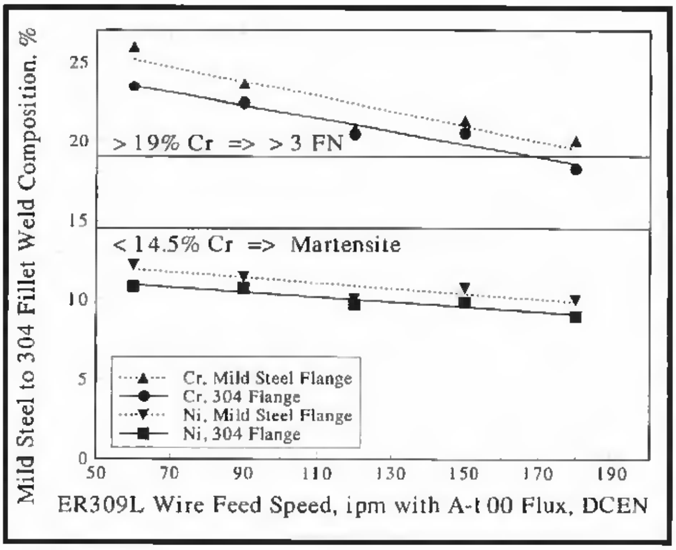

Fig. 16 — Effect of wire feed speed on fillet weld chromium and nickel contents in DCEN welds with the chromium-adding flux.

significantly larger contributor to dilution than does the web (see Fig. 4, for example). This is simply the result of asymmetric geometry below the root of a fillet weld. Second, even though the fillet weld surfaces show no evidence of magnetic arc blow, a clear tendency was noted for the root penetration to deflect toward the mild steel side of the joint. Figure 5 shows the progression of this second phenomenon with increasing wire feed speed in a series of welds where mild steel is the flange. Figure 6 compares two welds made under identical conditions, except in one case the flange is mild steel while the web is 304 and in the other case the web is mild steel while the flange is 304. The weld surfaces show no asymmetry about the joint axis, but the penetration in each case is asymmetric, deflected toward the mild steel side. This asymmetric penetration may be driven by Marangoni surface tension effects as explained by Heiple and Roper (Ref. 10), but as can be seen in Table 1, there is not a large difference in sulfur content between the mild steel and 304 base metals used in this study. A surface tension difference between mild steel and 304 may still explain the effect, or the effect may be caused by a magnetic deflection of the hot metal convection currents in the weld pool toward the mild steel side. At any rate, the penetration deflection is consistently toward the mild steel side for all of the DCEP welds.

Figure 7 summarizes the dilution measurements for DCEP welding with the chromium-compensating flux. Total dilution increases with increasing wire feed speed (increasing current), and total dilution at any given wire feed speed is little affected by whether the flange is mild steel or 304 stainless. However, the dilution contribution from the mild steel side of the joint is strongly affected by whether the flange is mild steel or 304 stainless. When the flange is mild steel, both the asymmetric geometry and the asymmetric penetration tendency favor more dilution from the mild steel, so di-

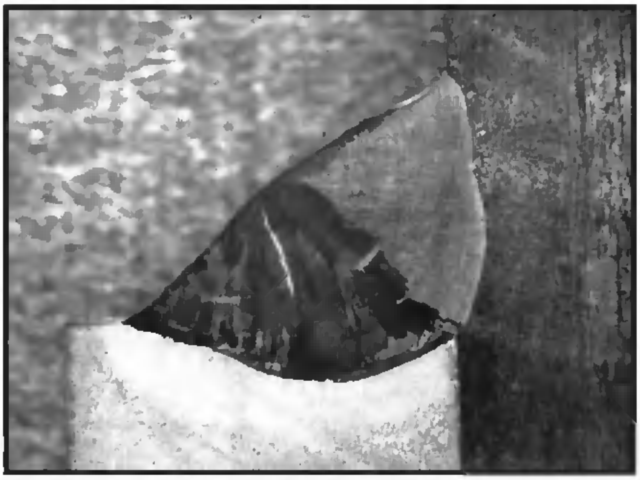

Fig. 17 — Photomacrograph of cross section of fillet weld BWF140. Note the subsurface hot crack. This weld measured only 0.8 FN.

lution from the mild steel side increases strongly with increasing wire feed speed. However, when the web is the mild steel, the asymmetric geometry effect tends to cancel out the asymmetric penetration effect, so the mild steel contribution to dilution is not strongly influenced by wire feed speed.

Figure 8 summarizes the fillet weld chromium and nickel contents as functions of wire feed speed for DCEP welding with the chromium-compensating flux. Both chromium and nickel contents decrease with increasing wire feed speed (due to increasing dilution). The decreases are steeper when the flange is mild steel, as compared to when the flange is 304 stainless steel. Welds with less than 19% Cr have less than 3 FN (Table 3) and may be sensitive to hot cracking. Welds with less than about 14.5% Cr contain extensive amounts of martensite. Hardness measurements on a few of these welds showed that the highly martensitic welds are about 38 Rockwell C, while the highly austenitic welds are well below 20 Rockwell C. Bend tests in a cladding study of welds with similar compositions (Ref. 9) showed conclusively that such martensitic welds are brittle, while the highly austenitic welds are ductile (if free from hot cracks).

The situation is better when DCEP welding is performed with the chromium-adding flux, due to its ability to add chromium to the weld. The dilution behavior vs. wire feed speed (Fig. 9) for this situation is virtually identical to that when the chromium-compensating flux is used DCEP (Fig. 7). However, the deposit chromium content is higher with the chromium-adding flux, so welds made at lower wire feed speed have greater than 19% Cr and ferrite content above 3 FN. Again, a mild steel flange makes the situation more difficult than a 304 flange. Figure 10 shows graphically the deposit chromium and nickel contents for DCEP welding with the chromium-adding flux. Comparison with Fig. 8 (chromium-compensating flux with DCEP) shows that the nickel results are virtually identical for the two fluxes, but the deposit chromium is always shifted to higher levels with the chromium-adding flux (due to the flux chromium content). Again, the deposit chromium and nickel contents decrease with increasing wire feed speed at a greater rate when mild steel is the flange than when 304 is the flange.

The penetration situation is much different when welding is performed DCEN. Figure 11 shows the series of welds made with the highly basic chromium-free flux, all with mild steel flanges, at increasing wire feed speeds. The deep penetration into the root of DCEP welding, at high wire feed speeds, is completely absent in these DCEN welds. Even at the highest wire feed speed considered, the penetration extends only slightly beyond the original root. There is still asymmetric penetration, as exemplified by Fig. 12, but now the penetration is consistently greater toward the web, regardless of whether the web is mild steel or 304. This is clearly not due to a Marangoni surface tension effect. It seems likely that the DCEN penetration asymmetry is caused by the web constituting a smaller heat sink than the flange, because the web only permits heat flow in one direction while the flange permits heat flow in two directions.

That the penetration into the web is greater than that into the flange for DCEN welding is demonstrated by the dilution vs. wire feed speed plot of Fig. 13, for the highly basic chromium-free flux. Dilution from mild steel is consistently greater

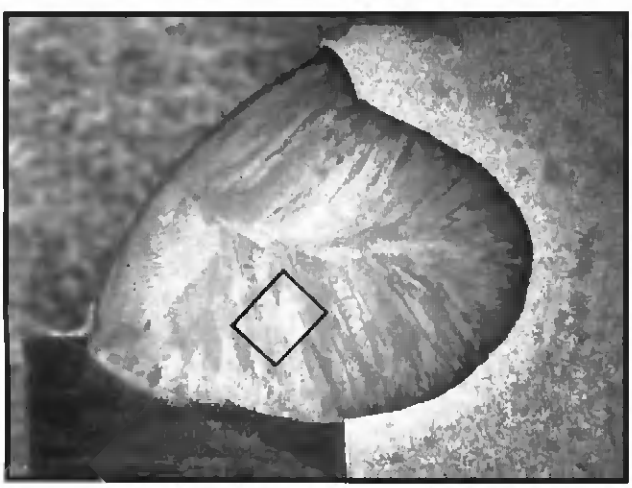

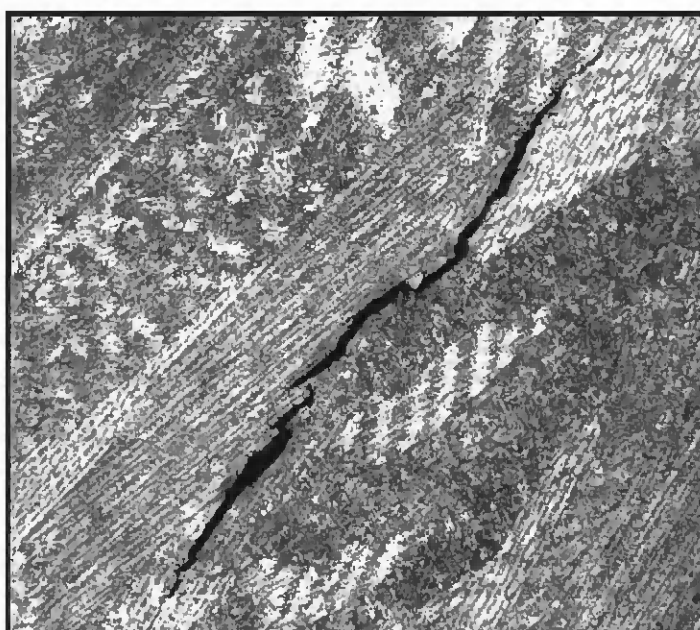

Fig. 18 — Cross section of fillet weld BWF111. The right view is a 50X magnification of the rectangle marked in the photomacrograph at left. The hot crack along solidification grain boundaries is clearly evident in the 50X view. The weld measured a false 62 FN due to the high martensite content.

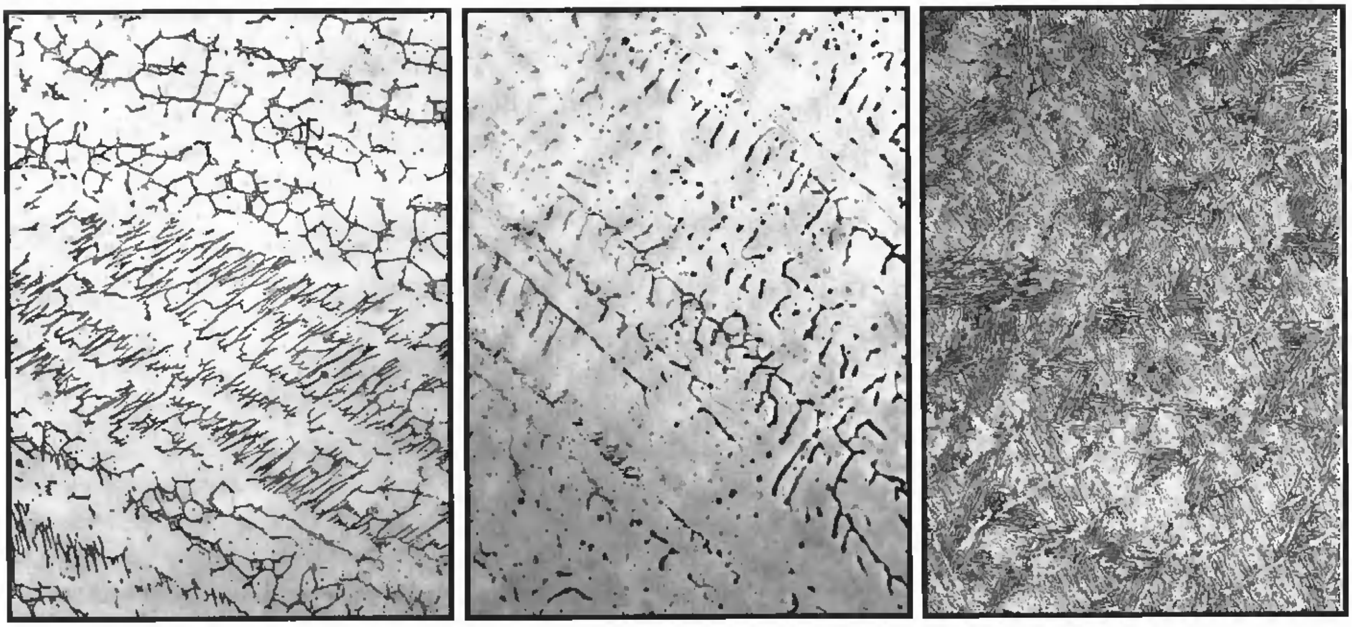

Fig. 19 — Typical weld microstructures (X500) of fillet welds: Left — BWF131, 10.6 FN; Center — BWF140, 0.8 FN; and Right — BWF111, 62 FN. The martensite in BWF111, which causes the false high 62 FN, is clearly visible in the right microstructure.

for a mild steel web (304 flange) than for a mild steel flange. Figure 14 presents the fillet weld chromium and nickel results. With the mild steel flange, several welds are above 19% Cr and above 3 FN, but with the mild steel web, none of the welds are above 19% Cr, or above 3 FN. However, in no case is dilution high enough to cause martensite to form in the welds. Note also that the rate of decrease in deposit chromium, or deposit nickel, is virtually independent of whether the flange is mild steel or 304, in contrast to the situation in DCEP welding.

Greater penetration into the web than into the flange for DCEN welding is also observed for the chromium-adding flux at any given wire feed speed, as can be seen in Fig. 15. With the addition of considerable chromium from the flux, all of the welds, except for that at the highest wire feed speed with a mild steel web, are above 19% Cr and above 3 FN — Fig. 16. This combination of DCEN welding and the chromium-adding flux produced the broadest range of welding conditions that met these two criteria. In addition, none of these welds contained martensite. As with DCEN welding with the highly basic chromium-free flux, the rate of decrease of deposit chromium, or nickel, is virtually independent of whether the flange is mild steel or 304. As noted earlier, undercut was observed at the highest wire feed speed (highest travel speed).

Hot cracks were observed in some of the near-zero FN welds (which solidified as primary austenite) and in some of the high dilution, highly martensitic welds (which also solidified as primary austenite). Examples of these cracks are shown in Figs. 17 (near zero FN) and 18 (highly martensitic weld). In both cases, the cracks clearly follow solidification grain boundaries, which is typical of hot cracks. Both conditions would be unacceptable for most purposes. It should be noted that in neither hot crack example is the crack found to extend to the weld surface. In fact, none of the welds in this study had cracking visible from the weld surface. The cracks found in the cross sections would thus not be detected by visual examination. They might be found by ultrasonic examination, but interpretation of ultrasonic signals from dissimilar metal welds is difficult. Because only one cross section of each weld was examined, it is likely that not all cracked welds were detected in this study. On the basis of the observations of hot cracks herein, and in many other studies, it seems likely that many of the welds containing either very low ferrite, or substantial martensite, contain hot cracks somewhere within them.

Figure 19 shows representative weld deposit microstructures from this study. Shown on the left side of Fig. 19 is a typical microstructure of a weld that solidified as primary ferrite. No cracks were found in such welds, and none would be expected.

Shown in the center of Fig. 19 is a typical microstructure of a weld that solidified as primary austenite and contains a small amount of eutectic ferrite in the cell boundaries. Hot cracks were found in some welds of this microstructure.

The right side of Fig. 19 shows a typical microstructure of a weld that solidified as primary austenite and subsequently transformed extensively to martensite. Hot cracks were found in some welds of this microstructure. The martensite produced a false ferrite measurement of 62 FN. The hardness of this weld measured 38 Rockwell C.

Conclusions

This study has clearly demonstrated that the usual choice of Type 309L filler metal for joining mild steel to 304 (or other austenitic stainless steels) is not without considerable risk in SAW, but suitable welding conditions can be found. While SMAW with 309L filler metal will generally result in a fillet weld of at least 3 FN, indicating solidification as primary ferrite and therefore freedom from hot cracking, the higher dilution of SAW makes this much less certain. Many welds were produced that did not meet this criterion. On the basis of this study's results, the following conclusions are drawn for the application of submerged arc fillet welding, with ER309L welding wire, of mild steel to austenitic stainless steel such as Type 304:

1) With ER309L filler metal and low dilution from the mild steel side of the joint, fillet welds of 3 FN or more can be produced that are crack-free and ductile.

2) Higher dilution from the mild steel side of the joint can produce welds that are nearly fully austenitic at room temperature. These welds solidify as primary austenite and are likely to contain hot

cracks.

3) Still higher dilution from the mild steel side of the joint produces welds that are highly martensitic at room temperature. They are hard (about 38 Rockwell C) and not ductile.

4) Dilution increases with increasing wire feed speed (increasing current) using either DCEP or DCEN welding.

5) At a given wire feed speed (current), less dilution occurs in DCEN welding than in DCEP welding.

6) In DCEP welding, penetration asymmetry was observed in the direction of the mild steel side of the joint. This in turn tended to increase dilution from the mild steel into the weld, making ferrite-free or martensitic welds more likely.

7) In DCEP welding, the flange tends to contribute more heavily to the dilution than does the web, because the penetration is beyond the root and the base metal geometry is asymmetric below the root.

8) In DCEN welding, the penetration beyond the root is minimal. In this case, the penetration tends to be greater on the web side of the joint than on the flange side of the joint. As a result, a mild steel web is less tolerant to dilution than is a 304 web.

9) With each flux, some welds were produced that were crack-free and consisted of austenite with some ferrite. However, the chromium-adding flux offered the broadest range of welding conditions that did not result in martensite or cracking.

Acknowledgments

The assistance of John Wijnen and of John McLane, in preparing the many metallographic cross sections for this study and carrying out the dilution measurements, is gratefully acknowledged.

References

1. American Welding Society. 1982. *Welding Handbook*, 7th ed., Vol. 4, Chapter 12, pp. 527–528, American Welding Society, Miami, Fla.

2. Folkhard, E. 1988. *Welding Metallurgy of Stainless Steels*, pp. 231–235, Springer-Verlag, Wein, New York.

3. Thielsch, H. 1952. Stainless-steel weld deposits on mild and alloy steels. *Welding Journal* 31(1): 37-s to 64-s.

4. Lundin, C. D. 1982. Dissimilar metal welds — Transition joints literature review. *Welding Journal* 61(2): 58-s to 63-s.

5. Schaeffler, A. L. 1949. Constitution diagram for stainless steel weld metal. *Metal Progress* 56(11): 680–680B.

6. FERRITE PREDICTOR computer software, © 1992, American Welding Institute, Knoxville, Tenn.

7. Kotecki, D. J., and Siewert, T. A. 1992. WRC-1992 constitution diagram for stainless steel weld metals: A modification of the WRC-1988 diagram. *Welding Journal* 71(5): 171-s to 178-s.

8. Siewert, T. A., McCowan, C. N., and Olson, D. L. 1988. Ferrite Number prediction to 100 FN in stainless steel weld metal. *Welding Journal* 67(12): 289-s to 298-s.

9. Kotecki, D. J. 1996. Dilution control in single wire stainless steel submerged arc cladding. *Welding Journal* 72(2): 35-s to 45-s.

10. Heiple, C. R., and Roper, J. R. 1982. Mechanism for minor element effect on GTA fusion zone geometry. *Welding Journal* 61(4): 97-s to 102-s.